SOME EFFECTS OF ANISOTROPY ON THE WAVE PROPAGATION IN SATURATED POROUS MEDIA.

Hans van der Kogel [I)]
Joel Sweet [II)]

SUMMARY

Wave propagation in an anisotropic saturated porous solid is studied, particularly in an extended shear beam configuration. An equivalent of the consolidation equation is derived. Analytical results for the propagation of discontinuities are generated and these results are used to check the numerical scheme. Vertical propagating waves are studied using the numerical scheme and results show pore pressure generation due to anisotropy.

INTRODUCTION

Wave propagation through saturated porous media attains the attention of research workers in different fields. The main objective of geophysicists is to determine the structure of geological profiles by wave reflection methods. The current number of papers shows the upsurge of interest in the multi phase dynamics, e.g. (1), (2). Most of the geophysical work deals with the linear theory. Research work on military applications shows a continuous interest in the question of explosion-induced liquefaction of soils (3). In this field one usually considers the non-linear effects. In the field of earthquake engineering the role of pore pressure became more evident during the last decade. On one hand one considers the triggering of an earthquake by pore pressure generation (4), on the other hand the generation of pore pressure by the earthquake itself can be signiticant(5), (6).

In this paper we address ourselves to the latter. Although some papers have appeared on isotropic saturated solids (7) - (9), much less is known about the behaviour of anisotropic saturated elastic solids (10). We focuss our attention here on the so called shear beam configuration, however we also allow for expansion or contraction during shear of the porous solid material. First we pose the fieldequations, based on the balance equations and constitutive relations. Hereafter we derive some analytical results for reasons of relating to well known results and checking the numerical scheme for the fieldequations.

The numerical approach we utilize in this study is the non-linear two-phase finite element code, SATPILE (11). Whereas the generality of this non-linear code allows for one-, two- or three-dimensional configurations as well as dynamic or static response, we limit ourselves here to one spatial dimension and a linear dynamic wave propagation environment. The numerical technique is verified by comparing numerical solutions to their theoretical counterparts. We have also used the SATPILE code to investigate the generation of pore pressure resulting from a SH-wave earthquake boundary condition. For this study we have used the north-south component of the 1940 El Centro earthquake record to excite a 80 meter thick anisotropic saturated soil. The effect of both permeability and anisotropy amounts on the generation of pore pressure is investigated for this linear configuration.

A. FIELDEQUATIONS.

We consider an anisotropic linear elastic porous solid material in a two dimensional configuration with orthogonal coordinates x and y. Furthermore we assume that the boundary conditions are such that the variables are independent of y. Then we can write:

$$\sigma_{xx} = A \frac{\partial u_x}{\partial x} + D \frac{\partial u_y}{\partial x} \qquad (A.1)$$

$$\tau_{xy} = D \frac{\partial u_x}{\partial x} + F \frac{\partial u_y}{\partial x} \qquad (A.2)$$

where σ_{xx} is the normal stress on x-direction and τ_{xy} is the shear stress, u_x is the displacement in x-direction and u_y is the displacement in y-direction; A, D and F are constants.

I) Research Engineer; Delft Soil Mechanics Laboratory, Delft, Netherlands.
II) Consultant ; Coast analytics, Inc., Cal., U.S.A.

We assume that the porous solid is saturated with a compressible fluid. The storage equation for the fluid in the linear case is:

$$\frac{\partial w_x}{\partial x} + \frac{1-n}{n}\frac{\partial v_x}{\partial x} = -\frac{1}{K_w}\frac{\partial p}{\partial t} \qquad (A.3)$$

"Eq. (A.3)" states that the flux of solid material and fluid in a unit cell is compensated by a pressure change in the fluid. The average fluid velocity is denoted by w_x and the average solid velocity by v_x (both in x-direction), n is the porosity, p is the pore pressure and K_w is the compression modulus of the fluid.

We consider the following momentum equations for the fluid in the linearized case:

$$n\rho_w \frac{\partial w_x}{\partial t} = -n\frac{\partial p}{\partial x} - \frac{n^2}{k_{xx}}(w_x - v_x) - \frac{n^2}{k_{xy}}(w_y - v_y) \qquad (A.4)$$

$$n\rho_w \frac{\partial w_y}{\partial t} = -\frac{n^2}{k_{yy}}(w_y - v_y) - \frac{n^2}{k_{yx}}(w_x - v_x) \qquad (A.5)$$

Here we state that the inertia forces are balanced by pressure gradients (in x-direction) and Darcian interaction forces due to relative movement of the phases. The density of the fluid is denoted by ρ_w and the permeability coefficients by k_{xx}, $k_{yx} = k_{xy}$, and k_{yy}. In a similar way we derive the momentum balance equations for the grain structure:

$$(1-n)\rho_p \frac{\partial v_x}{\partial t} = \frac{\partial \sigma_{xx}}{\partial x} - (1-n)\frac{\partial p}{\partial x} + \frac{n^2}{k_{xx}}(w_x - v_x) + \frac{n^2}{k_{xy}}(w_y - v_y) \qquad (A.6)$$

$$(1-n)\rho_p \frac{\partial v_y}{\partial t} = \frac{\partial \tau_{yx}}{\partial x} + \frac{n^2}{k_{yy}}(w_y - v_y) - \frac{n^2}{k_{yx}}(w_x - v_x) \qquad (A.7)$$

The second term on the right hand side of the first equation is added because we assume here that the grainlike solid material is almost completely surrounded by the fluid. The density of the solid material is ρ_p.

Hence the set of "Eq. (A.1) to (A.7)" forms a linear system of seven equations with seven unknowns: v_x, v_y, w_x, w_y, σ_{xx}, τ_{xy} and p. The independent variables are x and t.

B. CONSOLIDATION

We will now derive the consolidation equation for the anisotropic saturated porous elastic solid. The fieldequations "Eq. (A.1)" to "Eq. (A.7)" without inertia terms, cross flow effects and compressible fluid reduce to:

$$\frac{\partial \sigma_{xx}}{\partial t} = A\frac{\partial v_x}{\partial x} + D\frac{\partial v_y}{\partial x} \qquad (B.1)$$

$$\frac{\partial \tau_{xy}}{\partial t} = D\frac{\partial v_x}{\partial x} + F\frac{\partial v_y}{\partial x} \qquad (B.2)$$

$$\frac{\partial w_x}{\partial x} + \frac{1-n}{n}\frac{\partial v_x}{\partial x} = 0 \qquad (B.3)$$

$$0 = -n\frac{\partial p}{\partial x} - \frac{n^2}{k_{xx}}(w_x - v_x) + n\rho_w g \qquad (B.4)$$

$$0 = -\frac{n^2}{k_{yy}}(w_y - v_y) \qquad (B.5)$$

$$0 = \frac{\partial \sigma_{xx}}{\partial x} - (1-n)\frac{\partial p}{\partial x} + \frac{n^2}{k_{xx}}(w_x - v_x) + (1-n)\rho_p g \qquad (B.6)$$

$$0 = \frac{\partial \tau_{xy}}{\partial x} + \frac{n^2}{k_{yy}}(w_y - v_y) \qquad (B.7)$$

We have also introduced gravity terms in x-direction for completeness(where g is the gravitational constant).

From "Eq. (B.5)" follows:

$$w_y = v_y \tag{B.8}$$

and from "Eq. (B.8)" and "Eq. (B.7)" follows:

$$\frac{\partial \tau_{xy}}{\partial x} = 0 \qquad \text{or} \qquad \tau_{xy} = A^*(t) \tag{B.9}$$

Hence when we know the shear stress at the boundary we know also the shear stress in the field. After some algebra (see Appendix I) we can prove:

$$K_p^* k_{xx} \frac{\partial^2 p}{\partial x^2} = \frac{\partial p}{\partial t} + \frac{\partial \sigma_t(o,t)}{\partial t} - \alpha \frac{\partial \tau_{xy}(o,t)}{\partial t} \tag{B.10}$$

where:

$$K_p^* = A - \frac{D^2}{F}$$

$$\alpha = \frac{D}{F}$$

$$A, F > o$$

We note that if D = o (no contraction or expansion during shear) "Eq. (B.10)" reduces to the well-known consolidation equation in soil mechanics (12). Thus, the effect of increasing D gives rise to an additional source term for the pore pressure in the whole field due to an applied shear stress at the boundary ($\alpha\, \tau_{xy}(o,t)$). It is also true that as D increases K_p^* decreases (thus raising the "consolidation time").

C. NUMERICAL STUDY

In order to validate the numerical technique, available theoretical solutions are reproduced using the discrete finite element formulation of the SATPILE code. We have limited our attention here to wave propagation effects. The first problem we consider is the isotropic configuration (D=o) where v_y and w_y both equal zero. The solution of this compressional configuration has been discussed by Garg et al. (13). The comparison of this theoretical solution to the SATPILE results appears in "Fig. 1" for two values of permeability. Except for the wave front dispersion unavoidable with discrete techniques, comparison with theory is excellent. The values of material parameters consistent with the notation of this study used to produce the results of "Fig. 1" are as follows:

$$\begin{aligned} \rho_w &= 0.672 \text{ g/cm}^3 \\ \rho_p &= 2.98 \text{ g/cm}^3 \\ n &= 0.27 \\ A &= .25 \times 10^{12} \text{ dyn/cm}^2 \\ F &= .099 \times 10^{12} \text{ dyn/cm}^2 \\ K_w &= .0127 \times 10^{12} \text{ dyn/cm}^2 \\ D &= 0 \\ \frac{n^2}{k} &= 0.219 \times 10^2;\ 0.219 \times 10^4 \text{ g/cm}^3 \text{ sec} \end{aligned} \tag{C.1}$$

where $k = k_{xx}$ and $\frac{1}{k_{xy}} = o$.

More complicated material configuration solutions can be validated if we introduce the concept of jump conditions at discontinuities and the speed of the discontinuities. These relationships are derived in Appendix II. The first case we consider is the special case when the continuum behaves as a single phase medium ($w_x = v_x$ and $w_y = v_y$). For this case the speed of the discontinuities is given by "Eq. (II.7)". Also, the jump in velocities are related by:

$$\frac{[v_y]}{[v_x]} = \frac{\rho U^2 - A - \frac{K_w}{n}}{D} \tag{C.2}$$

where brackets refer to jump values, U is the discontinuity speed and ρ is the composite density defined by:

$$\rho = (1-n)\rho_p + n\rho_w \tag{C.3}$$

For the numerical studies the following parameter values are utilized:

$$\rho_w = 1 \text{ g/cm}^3$$
$$\rho_p = 2.4285 \text{ g/cm}^3$$
$$n = 0.3$$
$$A = 2. \times 10^9 \text{ dyn/cm}^2 \qquad \text{(C.4)}$$
$$F = .5 \times 10^9 \text{ dyn/cm}^2$$
$$K_w = .75 \times 10^9 \text{ dyn/cm}^2$$
$$D = .5 \times 10^9,\ 1 \times 10^9 \text{ dyn/cm}^2$$
$$\frac{n^2}{k} = 10^6 \text{ g/cm}^3 \text{ sec}$$

The large value of $\frac{n^2}{k}$ was chosen along with the boundary conditions to produce a simple, single phase wave solution. Using the parameter values of "Eq. (C.4)"and "Eq. (II.7)", the values for U for the two values of D are as follows:

$$D = .5 \times 10^9 \text{ dyn/cm}^2\text{: } U = .0478 \times 10^6,\ .0138 \times 10^6 \text{ cm/sec;} \qquad \text{(C.5)}$$
$$D = 1 \times 10^9 \text{ dyn/cm}^2\text{: } U = .0487 \times 10^6,\ .0115 \times 10^6 \text{ cm/sec;}$$

For all cases a constant velocity boundary condition is applied at x = 0 in the y-direction equal to 1 cm/sec. The velocity boundary condition in the x-direction is determined from "Eq. (C.2)" using the smallest value for U from "Eq. (C.5)". The numerical solution for this case as given by "Fig. 2" is again excellent.

A more general configuration is now treated by allowing the fluid and solid velocities to differ for this case the discontinuity velocity is determined from "Eq. (II.6)". Also, the velocity discontinuities are related by:

$$\frac{[v_x]}{[v_y]} = \frac{(1-n)\rho_p U^2 - F}{D} \qquad \text{(C.6)}$$

$$\frac{[w_x]}{[v_y]} = \frac{(1-n)\ K_w}{D} \quad \frac{(1-n)\rho_p U^2 - F}{n\rho_w U^2 - nK_w} \qquad \text{(C.7)}$$

A numerical solution for this case appears in "Fig. 3" . The parameter values of "Eq. (C.4) with D = .5 x 10^9 dyn/cm^2 were utilized. The discontinuity velocity U equals:

$$U = .0217 \times 10^6,\ .0135 \times 10^6,\ .0479 \times 10^6 \text{ cm/sec.}$$

The solution in "Fig. 3" resulted from a velocity boundary condition for v_y equal to 1 cm/sec and boundary conditions for v_x and w_x determined from "Eq. (C.6), (C.7)" with U = .0217 x 10^6cm/sec. Again, a satisfactory numerical solution results. A simple wave shape has been produced by simulating $\frac{1}{k} = 0$. Having gained confidence in the SATPILE treatment of multiphase anisotropic behaviour, we will now investigate the pore pressure generation resulting from an earthquake-induced boundary condition. We are not, of course, attempting to predict a particular earthquake behaviour. Instead, we only seek to learn if the anisotropic representation as given by "Eq. (A.1) - (A.7)" can produce significant excess pore pressures by itself. The boundary condition we prescribe is a time varying velocity boundary condition for both v_y and w_y at some depth h with a stress-free condition at the top surface. The vertical velocities at depth h (v_x and w_x) are both taken to be zero. Thus, for this case when D = 0 the solution consists entirely of SH-waves with no induced excess pore pressures. The velocity time history we have utilized is the north-south component of the 1940 El Centro Earthquake "Fig. 4". This velocity is applied at a depth of 80 meters to a uniform material with values for n, ρ_w,ρ_p, A, F and K_w identical with "Eq. (C.4)". The isotropic (D = 0) single phase ($\frac{1}{k}$: "large") shear stress solution at a depth of 20 meters appears in "Fig. 5". The solution at this depth for the excess pore pressure and shear stress for the case D = .5 x 10^9 dyn/cm^2 and $k_{xx} = k_{yy} = 100$ cm^3 sec/g appears in "Fig. 6". The terms $\frac{1}{k_{xy}}$ and $\frac{1}{k_{yx}}$ are zero. Solutions with k varying between .01 and 1000 cm^3 sec/g are nearly identical to the results of "Fig. 6"; i.e. little two-phase behaviour for the first 20 seconds of time. Also, the induced pore pressure appears to be nearly linearly related to the value of $\frac{D}{F}$.

ACKNOWLEDGEMENT

A part of the work reported in this paper was supported by a grant of the Delft Soil Mechanics Laboratory, No. SE-680233.

APPENDIX I

Derivation of the diffusion equation.

Consider the fieldequations (A.1) to (A.7):

$$(I.1)\quad \frac{\partial \sigma_{xx}}{\partial t} = A\frac{\partial v_x}{\partial x} + D\frac{\partial v_y}{\partial x}$$

$$(I.2)\quad \frac{\partial \tau_{xy}}{\partial t} = D\frac{\partial v_x}{\partial x} + F\frac{\partial v_y}{\partial x}$$

$$(I.3)\quad \frac{\partial w_x}{\partial x} + \frac{1-n}{n}\frac{\partial v_x}{\partial x} = 0$$

$$(I.4)\quad 0 = -n\frac{\partial p}{\partial x} - \frac{n^2}{k_{xx}}(w_x - v_x) + n\rho_w g$$

$$(I.5)\quad 0 = -\frac{n^2}{k_{yy}}(w_y - v_y)$$

$$(I.6)\quad 0 = \frac{\partial \sigma_{xx}}{\partial x} - (1-n)\frac{\partial p}{\partial x} + \frac{n^2}{k_{xx}}(w_x - v_x) + (1-n)\rho_p g$$

$$(I.7)\quad 0 = \frac{\partial \tau_{xy}}{\partial x} + \frac{n^2}{k_{yy}}(w_y - v_y)$$

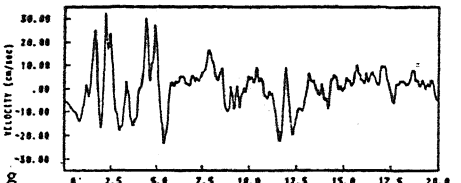

FIGURE 4. Velocity Time History for the North-South Component of the 1940 El Centro Earthquake.

Elimination of $\frac{\partial v_y}{\partial x}$ in (I.1) and (I.2) gives:

$$\frac{\partial \sigma_{xx}}{\partial t} = (A - \frac{D^2}{F})\frac{\partial v_x}{\partial x} + \frac{D}{F}\frac{\partial \tau_{xy}}{\partial t}(t) \qquad (I.8)$$

where we indicated that τ_{xy} is only a function of time (see conclusion "Eq. B.9)". From (I.4) follows:

$$\frac{\partial}{\partial x}(w_x - v_x) = -\frac{k_{xx}}{n}\frac{\partial^2 p}{\partial x^2} \qquad (I.9)$$

and from (I.3) follows:

$$\frac{\partial}{\partial x}(w_x - v_x) + \frac{1}{n}\frac{\partial v_x}{\partial x} = 0 \qquad (I.10)$$

Substitution of (I.9) into (I.10) gives:

$$\frac{k_{xx}}{n}\frac{\partial^2 p}{\partial x^2} = \frac{1}{n}\frac{\partial v_x}{\partial x} \qquad (I.11)$$

From (I.11) and (I.8) follows:

$$\frac{\partial \sigma_{xx}}{\partial t} = (A - \frac{D^2}{F})k_{xx}\frac{\partial^2 p}{\partial x^2} + \frac{D}{F}\frac{\partial \tau_{xy}}{\partial t}(t) \qquad (I.12)$$

adding (I.4) and (I.6) gives:

$$\frac{\partial}{\partial x}(-\sigma_{xx} + p) = n\rho_w g + (1-n)\rho_p g \qquad (I.13)$$

or:

$$-\sigma_{xx} + p = \left\{n\rho_w g + (1-n)\rho_p g\right\} x - \sigma_t(t) \qquad (I.14)$$

Substitution of (I.14) into (I.12) gives:

$$\frac{\partial p}{\partial t} + \frac{\partial \sigma_t(t)}{\partial t} = (A - \frac{D^2}{F})\, k_{xx} \frac{\partial^2 p}{\partial x^2} + \frac{D}{F} \frac{\partial \tau_{xy}(t)}{\partial t} \qquad (I.15)$$

or:

$$(A - \frac{D^2}{F})\, k_{xx} \frac{\partial^2 p}{\partial x^2} = \frac{\partial p}{\partial t} + \frac{\partial \sigma_t(t)}{\partial t} - \frac{D}{F} \frac{\partial \tau_{xy}(t)}{\partial t} \qquad (I.16)$$

The above equation is the one-dimensional "diffusion equation" for a porous linear elastic material that contracts or expands during shear and which is saturated with an incompressible fluid (including gravity effects).

APPENDIX II

Derivation of jump conditions and speed of discontinuities.

The jumpconditions are derived in the traditional way, that is to say we write the fieldequations in integral form and suppose that there exists a discontinuity propagating with U. As an example we treat here the first equation of the fieldequations A.1 to A.7.

$$\frac{\partial \sigma_{xx}}{\partial t} = A \frac{\partial v_x}{\partial x} + D \frac{\partial v_y}{\partial x} \qquad (II.1)$$

We write the equation in integral form:

$$-\frac{d}{dt} \int_{x_1}^{x_2} \sigma_{xx}\, dx + \left[A\, v_x + D\, v_y\right] = 0 \qquad (II.2)$$

where the square brackets denote the jump in the variables:

$$\left[A\, v_x + D\, v_y\right] = A\, v_x\Big|_{x_2} + D\, v_y\Big|_{x_2} - A\, v_x\Big|_{x_1} - D\, v_y\Big|_{x_1} \qquad (II.3)$$

Assuming that $x_1 \to x_2$ and a discontinuity propagates with speed U we derive:

$$\left[A\, v_x + D\, v_y\right] = \frac{d}{dt} \int_{x_1}^{s(t)} \sigma_{xx}\, dx + \frac{d}{dt} \int_{s(t)}^{x_2} \sigma_{xx}\, dx$$

$$= \sigma_{xx}(\bar{s},t).\dot{s} - \sigma_{xx}(\overset{+}{s},t).\dot{s} + \int_{x_1}^{s(t)} \sigma_{xx_t}\, dx + \int_{s(t)}^{x_2} \sigma_{xx_t}\, dx$$

In the limit of $x_1 \to s(t)$ and $x_2 \to s(t)$ the last two integrals approach zero (if σ_{xx_t} is continuous) and hence:

$$\left[A\, v_x + D\, v_y\right] = -U\, [\sigma_{xx}] \qquad (II.4)$$

In a similar way we derive the jumpconditions for the other fieldequations:

$$\begin{aligned}
&U\, [\tau_{xy}] + [D\, v_x + F\, v_y] = 0 \\
&-U\, [p] + \left[K_w\, w_x + K_w \frac{1-n}{n} v_x\right] = 0 \\
&-U\, [\rho_w\, w_x] + [p] = 0 \\
&-U\, [\rho_w\, w_y] = 0 \\
&-U\, [(1-n)\rho_p\, v_x] + [-\sigma_{xx} + (1-n)p] = 0 \\
&-U\, [(1-n)\rho_p\, v_y] + [-\tau_{xy}] = 0
\end{aligned} \qquad (II.5)$$

After some algebra we obtain the speed of the discontinuities in terms of the parameters of the system:

$$
\begin{aligned}
&(1-n)^2\rho_p^2\rho_w U^6 \\
&+ \Big\{ - F\,(1-n)\rho_p\rho_w - K_w\,(1-n)^2\,\rho_p^2 \\
&- (1-n)^2\rho_p\rho_w K_w \frac{1-n}{n} - A\,(1-n)\rho_w\rho_p \Big\} U^4 \\
&+ \Big\{ F\,K_w\,(1-n)\rho_p + F(1-n)\rho_w K_w \frac{1-n}{n} \\
&+ K_w A\,(1-n)\rho_p + FA\,\rho_w - D^2\rho_w \Big\} U^2 \\
&+ \Big\{ - F\,K_w A + D^2 K_w \Big\} = 0
\end{aligned}
\qquad \text{(II.6)}
$$

A similar relationship can also be derived for the special case when the continuum behaves as a single phase medium ($w_x = v_x$ and $w_y = v_y$). For this case "Eq. (II.6)" becomes:

$$\rho^2U^4 - (A + \frac{K_w}{n} + F)\rho U^2 + (A + \frac{K_w}{n})F - D^2 = 0 \qquad \text{(II.7)}$$

where ρ is the composite density defined as:

$$\rho = (1-n)\rho_p + n\rho_w \qquad \text{(II.8)}$$

REFERENCES

1. Dutta, N.C. and Seriff, A.J., 1979, On White's model of attenuation in rocks with partial gas saturation, Geophysics, Vol. 44, No. 11, p. 1806-1812.
2. Stoll, R.D., 1979, Experimental studies of attenuation in sediments, J. Acoust. Soc. Am., Vol. 66, No. 4, p. 1152 - 1160.
3. Blouin, S, 1978, Liquefaction evidence observed in various explosive events, International workshop on blast-induced liquefaction, Maidenhead, U.K., p. 95 - 110.
4. Garg, S.K., Brownell, D.H., and Pritchett, J.W., 1977, Dilatancy-induced fluid migration and the velocity anomaly, Journal of Geophysical Research, Vol. 82, No. 5, p. 855 - 864.
5. Ghaboussi, J., and Dikmen, S.U., 1978, Liquefaction analysis of horizontally layerd sands, J.Geotech.Eng.Div., Vol. 104, No. GT3, p. 341 - 356.
6. Finn, W.D. Liam, 1980, Dynamic analysis of saturated cohesionless soils, Soils under cyclic and transient loading, Swansea, p. 549 - 550.
7. Biot, M.A., 1956, Theory of propagation of elastic waves in a fluid saturated porous solid, part I and part II, J.Acoust.Soc.Am., p. 158 - 191.
8. Ishihara, K., 1970, Approximate forms of wave equations for water saturated porous materials and related dynamic modulus, Soils and Foundations, Vol. 10, No. 4, p. 10 - 38.
9. Didukh, B.I. and Trifonov-Yakovlev, D.A., 1974, Development of a practical method of solving problems of the dynamics of saturated soil, translated from: Osnovaniya, Fundamenty i Mekhanika Gruntov, No. 4, p. 24 - 27.
10. Mengi, Y, and Mc. Niven, H.D., 1978, Propagation and decay of waves in porous media, J.Acoust.Soc.Am., Vol. 64, No. 4, p. 1125 - 1131.
11. Sweet, J. and Cecil, R., 1979, SATPILE, A finite element computer code that analyzes the non-linear behaviour of saturated (two-phase) continua and neighboring structural components, J.S.A.-79-014.
12. Scott, R.F., 1963, Principles of Soil Mechanics, Addison-Wesley.
13. Garg, S.K., Nayfeh, A.H., Good, A.J., Compressional waves in fluid saturated elastic porous media, J.Appl.Phys., Vol. 45, No. 5, p. 1968 - 1974.

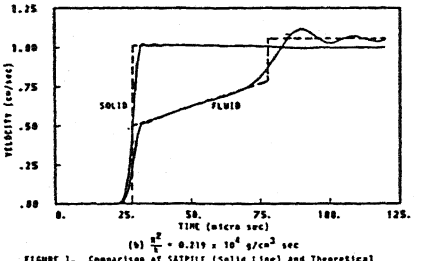

(b) $\frac{n^2}{k} = 0.219 \times 10^6$ g/cm^3 sec

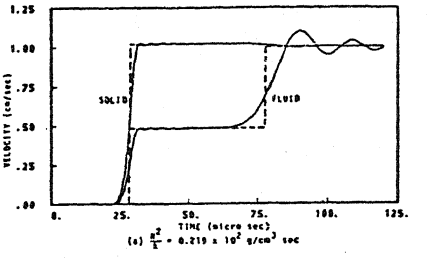

(a) $\frac{n^2}{k} = 0.219 \times 10^2$ g/cm^3 sec

FIGURE 1. Comparison of SATPILE (Solid Line) and Theoretical (Dashed Line) Results for a Prescribed Velocity Boundary Condition. Plotted are the Fluid and Solid Particle Velocities 10 cm from Boundary.

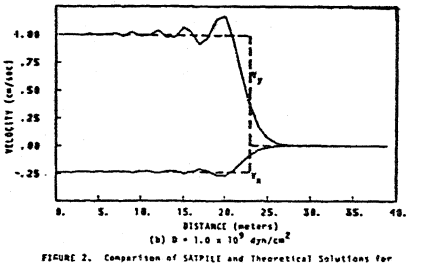

(b) $B = 1.0 \times 10^9$ dyn/cm^2

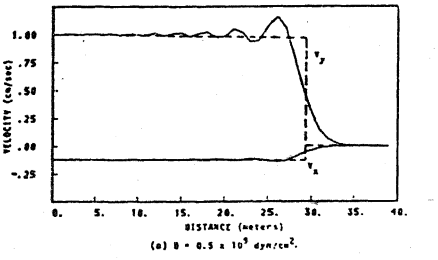

(a) $B = 0.5 \times 10^9$ dyn/cm^2.

FIGURE 2. Comparison of SATPILE and Theoretical Solutions for Axial (V_x) and Tangential Velocities (V_y). Problem Considered is Anisotropic Case Where Properties are Chosen to Result in Single-Phase Behavior.

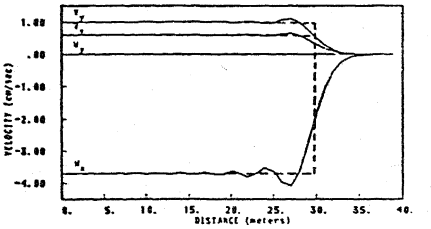

FIGURE 3. Comparison of SATPILE and Theoretical Solutions of the Velocities V_x, V_y, W_x and W_z for the Anisotropic Case of $B = 0.5 \times 10^9$ dyn/cm^2. Permeability was chosen so that 1/k Nearly Equals 0.

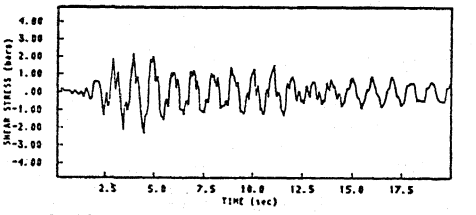

FIGURE 5. Shear Stress versus Time at a Depth of 20 meters for the Isotropic Case ($B = 0$). El Centro Horizontal Velocity Boundary Condition at a Depth of 20 meters is Utilized. Permeability was Chosen to be Small Enough to Prevent Two-Phase Behavior for the Time Considered.

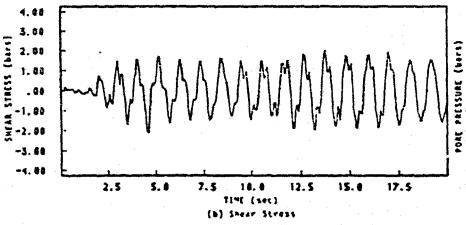

(b) Shear Stress

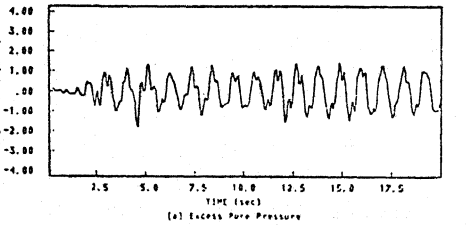

(a) Excess Pore Pressure

FIGURE 6. Excess Pore Pressure and Shear Stress versus Time at a Depth of 20 meters for the Anisotropic Case ($B = 0.5 \times 10^9$ dyn/cm^2) El Centro Boundary Condition again Utilized. Permeability (k) Equals 100 cm^{3}sec/g.